Energies **2013**, *6*, 3807-3821; doi:10.3390/en6083807

OPEN ACCESS

energies

ISSN 1996-1073

www.mdpi.com/journal/energies

Article

Flicker Mitigation by Speed Control of Permanent Magnet Synchronous Generator Variable-Speed Wind Turbines

Weihao Hu [1,*], Yunqian Zhang [1], Zhe Chen [1] and Yanting Hu [2]

[1] Department of Energy Technology, Aalborg University, Pontoppidanstraede 101, Aalborg DK-9220, Denmark; E-Mails: yqz@et.aau.dk (Y.Z.); zch@et.aau.dk (Z.C.)

[2] Electrical Engineering of the Institute of Art, Design and Technology, Glyndwr University, Wrexham LL11 2AW, UK; E-Mail: y.hu@glyndwr.ac.uk

* Author to whom correspondence should be addressed; E-Mail: whu@et.aau.dk; Tel.: +45-9940-3336; Fax: +45-9815-1411.

Received: 2 May 2013; in revised form: 23 July 2013 / Accepted: 23 July 2013 / Published: 29 July 2013

Abstract: Grid-connected wind turbines are fluctuating power sources that may produce flicker during continuous operation. This paper presents a simulation model of a MW-level variable speed wind turbine with a full-scale back-to-back power converter and permanent magnet synchronous generator (PMSG) developed in the simulation tool of PSCAD/EMTDC. Flicker emission of this system is investigated. The 3p (three times per revolution) power oscillation due to wind shear and tower shadow effects is the significant part in the flicker emission of variable speed wind turbines with PMSG during continuous operation. A new method of flicker mitigation by controlling the rotational speed is proposed. It smoothes the 3p active power oscillations from wind shear and tower shadow effects of the wind turbine by varying the rotational speed of the PMSG. Simulation results show that damping the 3p active power oscillation by using the flicker mitigation speed controller is an effective means for flicker mitigation of variable speed wind turbines with full-scale back-to-back power converters and PMSG during continuous operation.

Keywords: flicker; flicker mitigation speed controller; variable-speed wind turbine; permanent magnet synchronous generator (PMSG)

---

1. Introduction

During the past 20 years, renewable energy has become an increasing part of the worldwide power generation and especially wind energy has captured a significant part of this power production. As the wind power penetration into the grid is increasing quickly, the influence of wind turbines on the flicker is becoming an important issue. Flicker has been widely considered as a serious drawback and may limit the maximum amount of wind power generation that can be connected to the grid [1].

Variable speed wind turbines with multipole permanent magnet synchronous generator (PMSG) and full-scale back-to-back converters are becoming more popular worldwide, because of some of their advantages such as no need for a gearbox, high power density and easy control [2]. In this paper, a variable speed wind turbine with a PMSG and a full-scale back-to-back converter is chosen as the study case.

Flicker is induced by voltage fluctuations, which are caused by load flow changes in the grid. The flicker emission produced by grid-connected variable speed wind turbines with full-scale back-to-back converters during continuous operation is mainly caused by fluctuations in the output power due to wind speed variations, the wind shear and the tower shadow effects [3]. The wind shear and the tower shadow effects are normally referred to as the 3p oscillation, which means that three output power drops will appear per revolution for a three bladed wind turbine.

There are many factors that affect flicker emission of grid-connected wind turbines during continuous operation, such as wind characteristics and grid conditions [4–7]. Several methods have been proposed to mitigate the flicker from wind turbines. The most popular method is reactive power compensation. It can be realized by the grid side converter of variable speed wind turbines or the STATic COMpensator (STATCOM) connected at the point of common coupling (PCC) [8–13]. However, the flicker mitigation technique shows its limits, when the grid impedance angle is low in some distribution networks [14]. Also some papers focus on the use of active power control by varying the DC-link voltage of the full-scale converter to mitigate the flicker [15], but a big DC-link capacitor or the battery in the DC-link may be required in the method due to the storage of the fluctuation power in the DC-link.

A new control method for flicker mitigation by controlling the rotational speed is proposed in this paper. The 3p power oscillations from the wind turbine due to wind shear and tower shadow effects are actively damped by a flicker mitigation speed controller (FMSC), such that the flicker can be mitigated under any conceivable operation condition. When the FMSC damps the 3p active power oscillations which are the significant parts in the flicker emission, it smoothes the active power fluctuations into the grid by varying the rotational speed of the PMSG.

This paper is organized as follows: a simulation model and its control schemes of a MW-level variable speed wind turbine with a PMSG and a full-scale converter developed in PSCAD/EMTDC is presented in Section 2. Base on the wind turbine model, Section 3 investigates the flicker emission of this system during continuous operation. The FMSC which damps 3p active power oscillations due to wind shear and tower shadow effects is analyzed and designed in Section 4. Flicker mitigation is realized by speed control of variable speed wind turbines with PMSG in Section 5. Section 6 concludes this paper.

2. Wind Turbine Model and Control Schemes

2.1. Wind Turbine Model

The wind turbine considered here applies a PMSG, using a back-to-back full-scale PWM voltage source converter connected to the grid [2,15]. A complete wind turbine model includes the wind speed model, the aerodynamic model of the wind turbine, the mechanical model of the transmission system and models of the electrical components, namely the PMSG, PWM voltage source converters, transformer, and the control and supervisory system. Figure 1 illustrates the main components of the grid-connected wind turbine.

Figure 1. Block diagram of a grid-connected wind turbine with a PMSG and a full-scale converter.

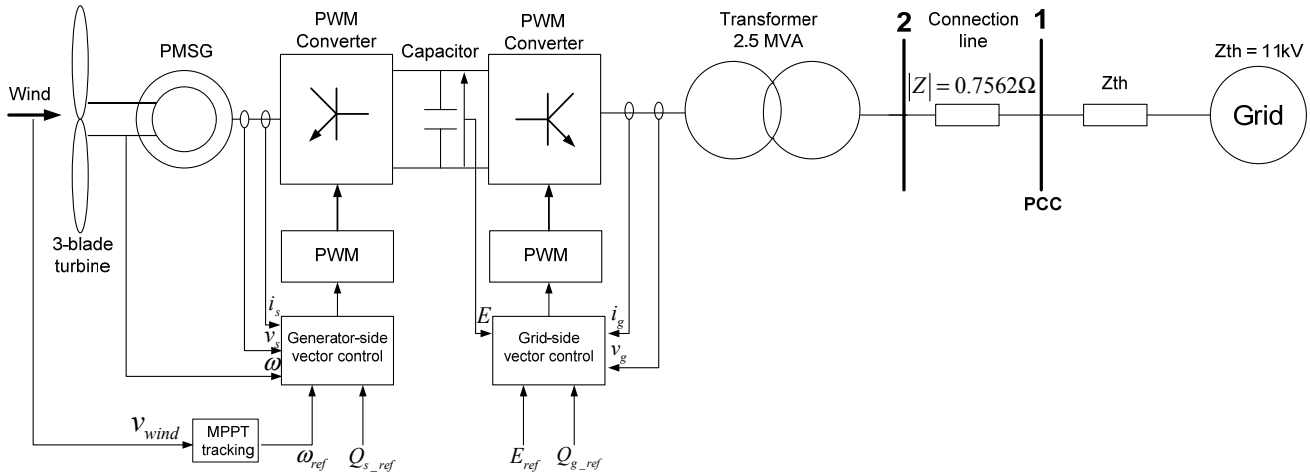

Wind simulation plays an important task in the wind turbine modeling. A wind model which is applied in this paper has been developed in [16]. The rotor wind model provides an equivalent wind speed for each wind turbine, which is conveniently used as an input to a simplified aerodynamic model of the wind turbine.

A simplified aerodynamic model is normally used when the electrical behavior of the wind turbine is the main interest of the study. The relation between the wind speed and aerodynamic torque may be described by the following equation:

$$Tw = \frac{1}{2}\rho\pi R^3 v_{eq}^2 \frac{C_P(\delta,\lambda)}{\lambda} \tag{1}$$

where Tw is the aerodynamic torque extracted from the wind (Nm); ρ is the air density (kg/m^3); R is the wind turbine rotor radius (m); v_{eq} is the equivalent wind speed (m/s); δ is the pitch angle of the rotor (degree), $\lambda = \omega R / v_{eq}$ is the tip speed ratio; ω is the wind turbine rotor speed (rad/s); and C_p is the aerodynamic efficiency of the rotor.

3p torque oscillations are important parts in the aerodynamic model. A comprehensive yet pragmatic model of 3p torque oscillations due to wind shear and tower shadow effects has been developed for a three-blade wind turbine [17], which is applied in this paper. Based on this model, the

equivalent wind speed (v_{eq}) will have three components. The first (v_{eq_0}) is the hub height wind speed, the second ($v_{eq_{ws}}$) is due to the wind shear, and the third ($v_{eq_{ts}}$) is due to the tower shadow. Therefore, the equivalent wind speed can be expressed as Equation (2) whose components are shown as Equations (3)–(5):

$$v_{eq} = v_{eq_0} + v_{eq_{ws}} + v_{eq_{ts}} \tag{2}$$

$$v_{eq_0} = V_H \tag{3}$$

$$v_{eq_{ws}} = V_H\left[\frac{\alpha(\alpha-1)}{8}\left(\frac{R}{H}\right)^2 + \frac{\alpha(\alpha-1)(\alpha-2)}{60}\left(\frac{R}{H}\right)^3 \cos 3\beta\right] \tag{4}$$

$$v_{eq_{ts}} = \frac{mV_H}{3R^2}\sum_{b=1}^{3}\left[\frac{a^2}{\sin^2\beta_b}\ln\left(\frac{R^2\sin^2\beta_b}{x^2}+1\right) - \frac{2a^2R^2}{R^2\sin^2\beta_b + x^2}\right] \tag{5}$$

where V_H is the wind speed at hub height (m/s), α is the empirical wind shear exponent, H is the elevation of rotor hub (m), β is the azimuthal angle of the blade (degree), β_b is respectively the azimuthal angle of each blade (degree), a is the tower radius (m), x is the distance from the blade origin to the tower midline (m), and $m = \left[1 + \frac{\alpha(\alpha-1)R^2}{8H^2}\right]$ is a coefficient of the wind turbine.

Only the drive train is considered in the mechanical model, while the other parts of the wind turbine structure, e.g., tower and flap bending modes, are neglected. The drive train model consists of the inertia of both the turbine and the generator. The connecting shaft is modeled as a spring and a damper [18]. The drive train model is shown in Figure 2. The equations for the drive train are:

$$J_w\frac{d\omega_w}{dt} = T_w - K_s\theta - D_s(\omega_w - \omega_g) \tag{6}$$

$$J_g\frac{d\omega_g}{dt} = K_s\theta + D_s(\omega_w - \omega_g) - T_e \tag{7}$$

$$\frac{d\theta}{dt} = \omega_w - \omega_g \tag{8}$$

where J_w is moment inertial of the wind turbine (kg·m^2); J_g is moment inertial of the generator (kg·m^2); K_s is stiffness coefficients of the shaft (kg·m^2·s^{-2}); D_s is damping coefficient of the shaft (kg·m^2·s^{-1}); ω_w and ω_g are the angular speed of the wind turbine and the generator (rad/s), respectively; θ is the angular displacement between the two ends of the shaft (rad).

Figure 2. The drive train model.

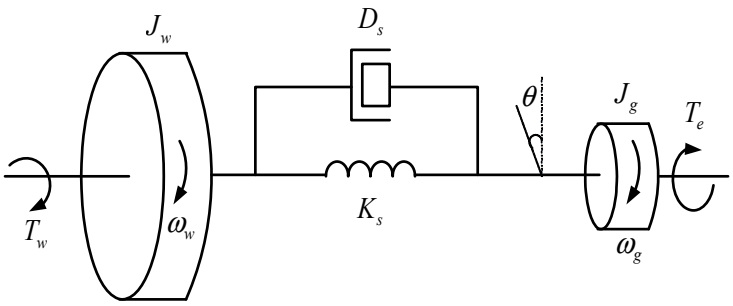

PSCAD/EMTDC software library provides a model of PMSG. In this paper, the PMSG model with detailed description of the stator direct and quadrature axis currents, the magnetic strength and the rotor speed is applied, using generalized machine theory [19]. Since the study interest is not concentrated on the switches of the PWM converter, an average model without switches is used so that the simulation can be carried out with a larger time step resulting in a simulation speed improvement [20].

2.2. Control Schemes

For a variable speed wind turbine with a PMSG and a back-to-back full-scale converter, it is possible to control the electromagnetic torque at the generator directly, so that the speed of the turbine rotor can be varied within certain limits. An advantage of the variable speed wind turbine is that the rotor speed can be adjusted in proportion to the wind speed in low to moderate wind speeds so that the optimal tip speed ratio is maintained. At this tip speed ratio the aerodynamic efficiency, C_P, is at maximum, which means that the energy conversion is maximized. It is normally referred to as maximum power point tracking (MPPT) [21].

In general, variable speed wind turbines may have two different control goals, depending on the wind speed. In low to moderate wind speeds, the control goal is maintaining a constant optimum tip speed ratio for maximum aerodynamic efficiency. In high wind speeds, the control goal is to keep the rated output power in order not to overload the system. For wind speeds above the rated value, the pitch control scheme limits the output power [22]. Reference [7] illustrates a relationship between the pitch angle and the wind speed, which is adopted in this paper.

Vector control techniques have been well developed for PMSG using back-to-back PWM converters [23–28]. Two vector control schemes are designed respectively for the generator-side and grid-side PWM converters, as shown in Figure 1.

3. Flicker Emission

This section is concentrated on the flicker emission of variable speed wind turbines with back-to-back full-scale converters and PMSG. The flicker emission produced by grid-connected variable speed wind turbines with PMSG and full-scale converter during continuous operation is mainly caused by fluctuations in the output active power. The studied system of variable speed wind turbines with PMSG is shown in Figure 1 and the parameters of the variable speed wind turbine are in the appendix (Table A1). The level of flicker is quantified by the short-term flicker severity P_{st}, which is normally measured over a ten-minute period. According to IEC standard IEC 61000-4-15 [29], a flickermeter model is built to calculate the short-term flicker severity P_{st} [3]. The equivalent wind speed, the rotor speed and the output active power of the wind turbine are shown in Figure 3.

When the mean wind speed is 10 m/s, the turbine speed may be around 15.5 rpm, which has a 3p oscillation frequency of 0.775 Hz. A frequency analysis of the equivalent wind speed and the output active power has been carried out, as shown in Figure 4. The spectrum of the equivalent wind speed shows that the 3p frequency component, due to the wind shear and the tower shadow effects, has been represented in the wind turbine model introduced in Section 2. Based on the model of wind shear and tower shadow, the higher frequency components, such as 6p, 9p, 12p, *etc.* are also included. The 3p oscillation frequency component is transmitted to the output active power of the wind turbine, which

will induce voltage fluctuation and flicker in the grid. The 3p oscillation due to the wind shear and the tower shadow effects is the significant part in the flicker emission of variable speed wind turbines with PMSG during continuous operation [15]. Flicker mitigation may be realized by damping the 3p oscillation in the output active power using appropriate control schemes.

Figure 3. The equivalent wind speed, the rotor speed and the output active power of the wind turbine.

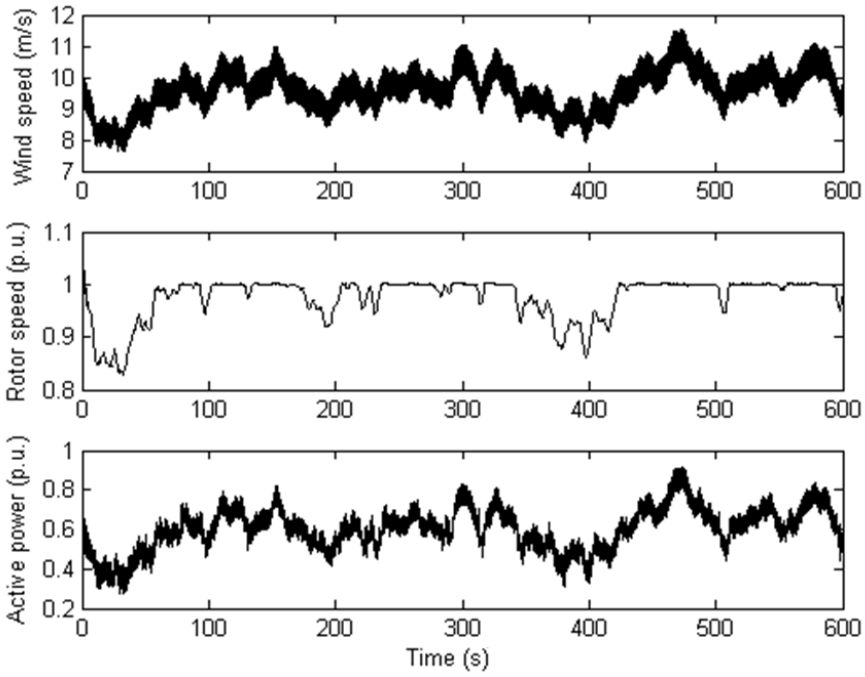

Figure 4. Power spectral density (PSD) of equivalent wind speed and output active power of the wind turbine.

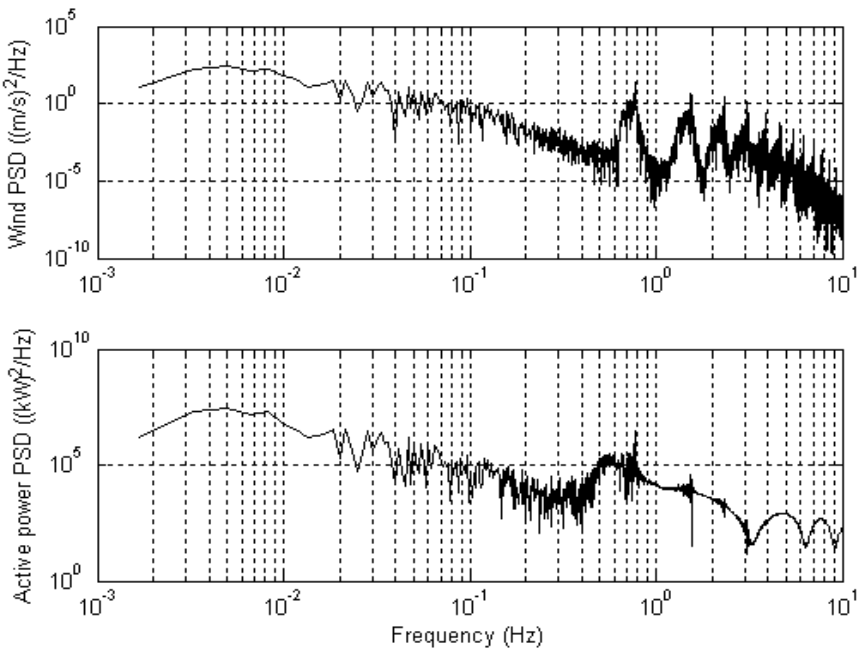

4. Flicker Mitigation by Speed Control

This section is concentrated on flicker mitigation of variable speed wind turbines with back-to-back full-scale converters and PMSG during continuous operation by speed control. Vector control techniques have been well developed for generator-side PWM converter [23–28]. The objective of the vector-control scheme for the generator-side PWM converter is to control the optimal power tracking for maximum energy capture from the wind by adjusting the speed of the wind turbine. The block diagram of the vector-control scheme for the generator-side PWM converter is shown in Figure 5, where ω_{ref} and ω_f are the reference value and the feedback value of the rotational speed; i_{dref} and i_{qref} are the reference values of direct and quadrature axis currents; i_d and i_q are the feedback values of direct axis and quadrature axis currents; θ is the phase angle of the rotor; T_w is the aerodynamic torque extracted from the wind.

Flicker mitigation may be realized by damping the 3p active power oscillation using the flicker mitigation speed controller (FMSC). In Figure 5, the FMSC loop is printed in grey blocks and lines to show how the FMSC is embedded in the control schemes of the generator-side PWM converter. The FMSC smoothes the 3p active power oscillations from wind shear and tower shadow effects of the wind turbine by varying the rotational speed of the PMSG.

The design objective of the FMSC is to damp 3p active power oscillations such that the flicker can be mitigated under any conceivable operating condition. To avoid that the FMSC interferes with the speed control of the wind turbine for normal operation, the active power signal of the generator need to be filtered with a bandpass (BP) filter before it enters into the FMSC.

Figure 5. Block diagram of the vector-control scheme for the generator-side PWM converter.

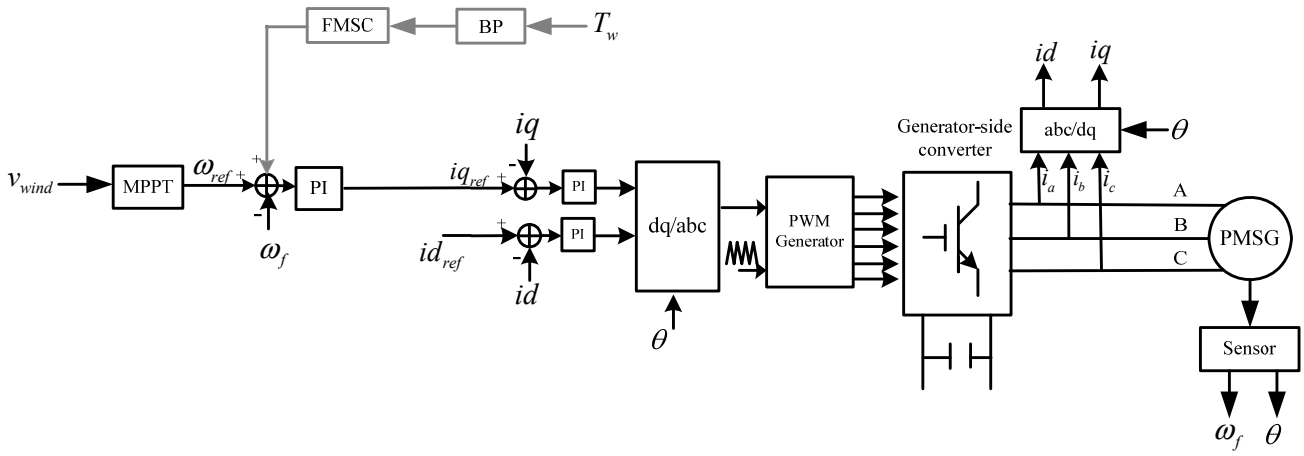

4.1. Design of BP Filter

The tasks of the BP filter are to only let the frequency of the 3p active power oscillation through and to block all other frequencies. Equation (9) shows a general transfer function of the BP filter:

$$F(s) = \frac{as^2 + bs + c}{ds^2 + es + f} \tag{9}$$

In most cases, the mean wind speed is from 5 to 20 m/s. The rotor speed of the wind turbine is from 7.5 to 15.5 rpm, which corresponds to 0.125 Hz to 0.258 Hz. So the 3p oscillation frequency is from 0.375 to 0.775 Hz. The average value of the 3p oscillation frequency is defined as the average 3p frequency (f_{3p}), which is 0.575 Hz in this study. The center frequency of BP filter is chosen as f_{3p} = 0.575 Hz to allow 3p oscillation frequencies pass the filter. By choosing an appropriate bandwidth, the BP filter allows the FMSC to act exclusively on 3p active power oscillations. The parameters of the BP filter are designed in Matlab [30], where the desired center frequency and the band width have to be specified. Figure 6 shows the bode plot of the BP filter. The designed parameters are $a = 0$, $b = 6$, $c = 0$, $d = 1$, $e = 6.007$ and $f = 13.25$.

Figure 6. Bode plot of the designed BP filter.

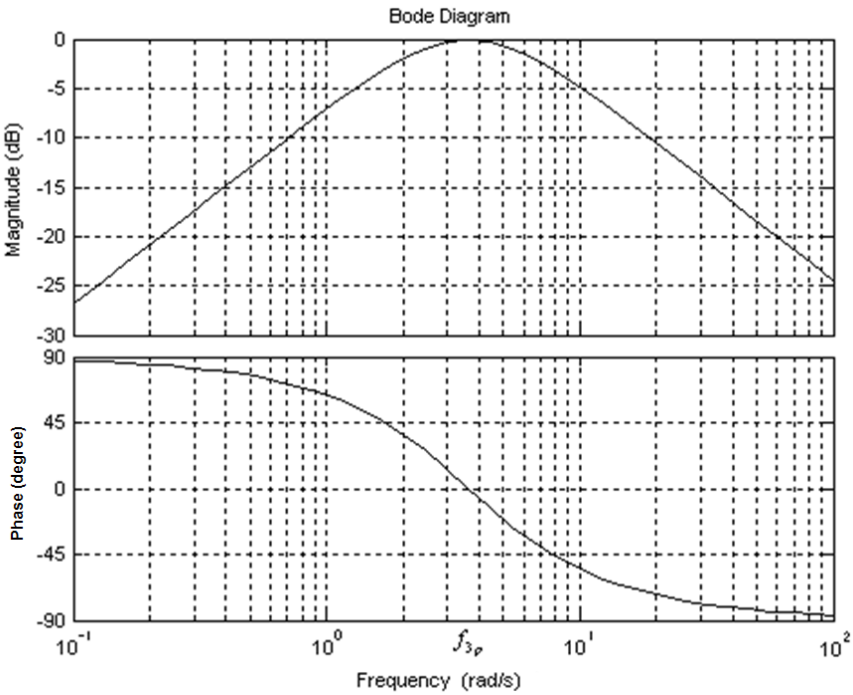

4.2. Design of FMSC

The FMSC has to produce a signal, which offsets the speed set point of the generator, ω_{ref} in Figure 5, such that ω varies in a way that energy from the 3p oscillations is stored in the wind turbine inertia. In other words, the measured torque oscillations of the wind turbine have to be translated to an oscillating speed offset with the right phase angle, which dampens the output active power oscillation to the grid. Equation (10) shows the relationship of the active power P_e, the electromagnetic torque T_e and the rotor speed ω_g of the generator:

$$P_e = T_e \omega_g \tag{10}$$

By permitting the generator speed to vary within a certain range, the power fluctuation of the generator could be suppressed when the power from the wind turbine is oscillating. The generator speed permitting range depends on the wind turbine inertia; it is −1%~+1% in this paper. Since the

varying range of generator speed is small, the fluctuation power of the generator is mainly determined by the fluctuation of the electromagnetic torque T_e.

Due to the small friction of the wind turbine drive train, the transfer functions of the mechanical drive train can be written as:

$$sJ_w\omega_w(s) = T_w(s) - K_s\theta(s) \tag{11}$$

$$sJ_g\omega_g(s) = K_s\theta(s) - T_e(s) \tag{12}$$

$$s\theta(s) = \omega_w(s) - \omega_g(s) \tag{13}$$

By assuming the fluctuation of the electromagnetic torque T_e could be controlled to zero at 3p frequency f_{3p}, the transfer function between the generator speed and wind turbine torque is:

$$\omega_g(s) = \frac{K_s}{J_w J_g s^3 + K_s(J_w + J_g)s} T_w(s) \tag{14}$$

This means that the electromagnetic torque T_e can be controlled to zero at 3p frequency f_{3p}, when the generator speed ω_g is controlled according to Equation (14) at 3p frequency f_{3p}. Figure 7 shows the bode plot of the transfer function between the generator speed and wind turbine torque.

Figure 7. Bode plot of the transfer function between the generator speed and wind turbine torque.

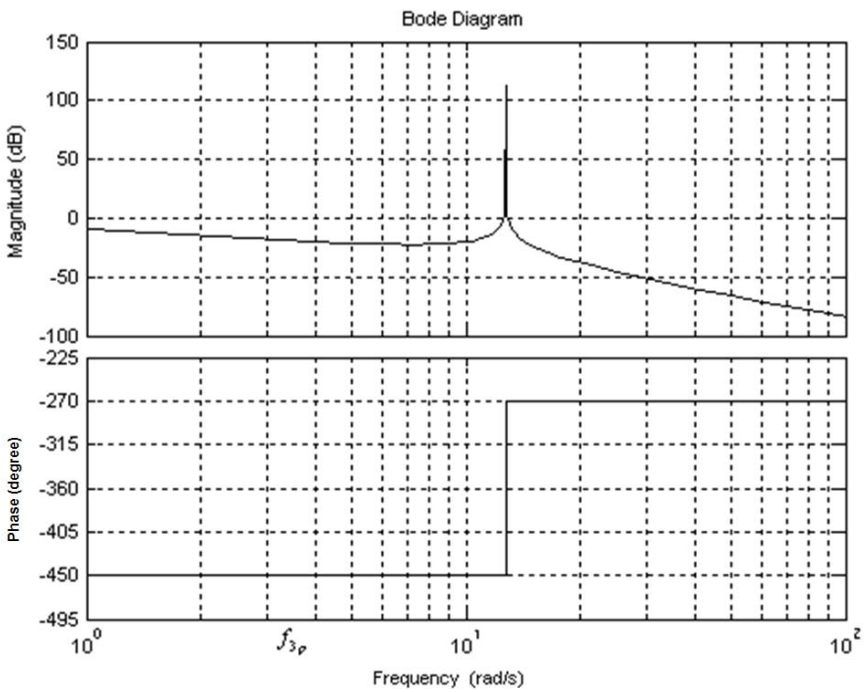

It can be concluded that the generator speed lags the wind turbine torque by 450° at 3p frequency f_{3p}, when the fluctuation of the electromagnetic torque of the generator is controlled to zero at f_{3p}. Hence, the signal in the FMSC path has to be delayed so that the fluctuation of the electromagnetic torque T_e is controlled to zero at f_{3p}. Since the BP filter does not cause any change in phase angle at f_{3p}, approximately, the angular contribution β of the FMSC for all 3p frequencies is:

$$\beta = -90^{\circ} + \varphi \tag{15}$$

where φ is the angle by which the generator speed ω_g lags the reference value of the generator speed ω_{ref} without the FMSC loop at f_{3p}. To find the required angular contribution β of the FMSC, the system is operated without the FMSC loop, and a sinusoidal disturbance signal that has frequency f_{3p} is superimposed on the reference value ω_{ref}. The angle φ by which ω_g lags the disturbance signal is measured. The angle φ may be also calculated by the transfer function of the whole system.

Equation (15) leads to the conclusion that the FMSC can be realized with a first-order lag element (PT1), which delays the phase by β at f_{3p}. Equation (16) shows the transfer function of a PT1:

$$F(s) = \frac{K_P}{1 + sT} \tag{16}$$

The angular contribution of a PT1 is:

$$\beta(\omega) = -\arctan(\omega T) \tag{17}$$

Hence, the time constant, T, of the PT1 can be calculated with the required angular contribution β at f_{3p}, as shown in Equation (18):

$$T = -\frac{\tan\beta}{\omega_{3p}} \tag{18}$$

where $\omega_{3p} = 2\pi f_{3p}$ is the average 3p angular speed.

The gain, K_P, of the PT1 can be tuned by testing, since the gain has no shift contribution in the FMSC loop. Increasing K_P increases the mitigation of the flicker; however, K_P has to be tuned such that the generator speed is within tolerable limits, which are −1%~+1% in this study. In the following section, the system operating under different conditions and the performance of the FMSC is accessed.

5. Flicker Mitigation Using FMSC

The flicker mitigation using FMSC is tested in many wind speed conditions. The variable speed wind turbine with PMSG and back-to-back full-scale converters are simulated with the FMSC as designed above. The parameters are the same as the ones in Section 3.

Figures 8 and 9 illustrate the short-term view and the long-term view of the wind turbine torque T_w, the generator rotational speed ω_g, the electromagnetic torque T_e and the active power to the grid. The wind turbine torque T_w is fluctuating due to the wind speed variations, the wind shear and tower shadow effects.

If the FMSC is not employed, the electromagnetic torque T_e and the active power to the grid will be the same as the wind turbine torque T_w, since the generator rotational speed is not controlled to vary according to the 3p components in the wind turbine torque Tw. From these figures, it can be seen that the electromagnetic torque T_e and the active power to the grid is smoothed by varying the generator rotational speed ω_g of PMSG when the FMSC is not adopted. As a consequence, the flicker is mitigated by reducing the output active power oscillations. However, the FMSC may only mitigate the flicker caused by 3p oscillations due to the wind shear and tower shadow effects which are the significant parts in the flicker emission.

Figure 8. Short-term view of the wind turbine torque, the generator rotational speed, the electromagnetic torque and the active power to the grid.

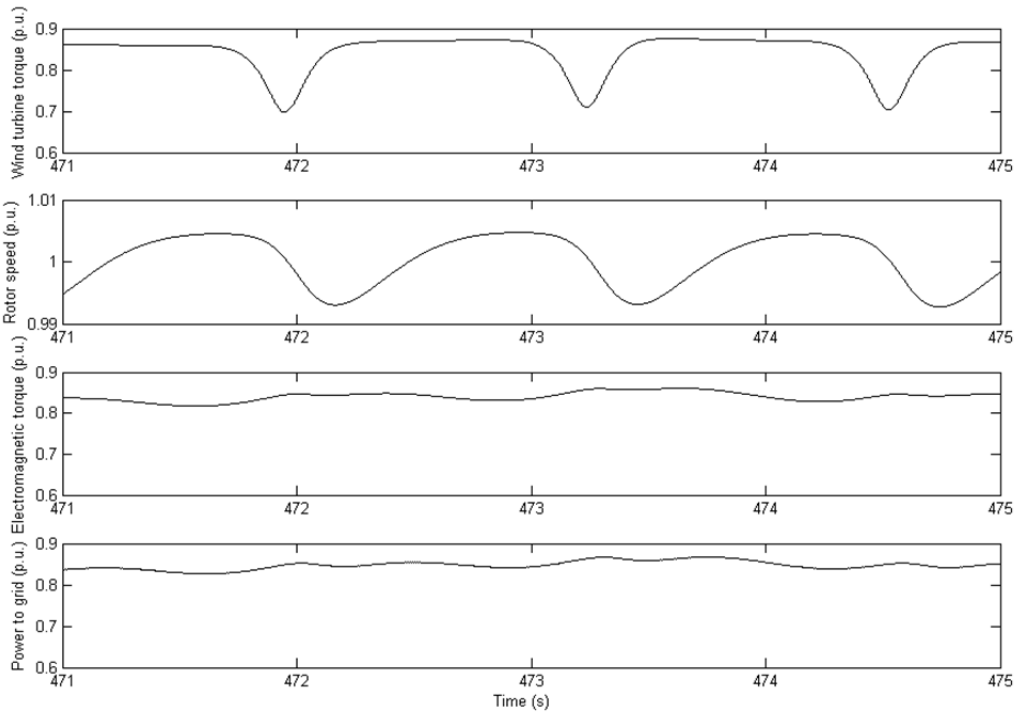

Figure 9. Long-term view of the wind turbine torque, the generator rotational speed, the electromagnetic torque and the active power to the grid.

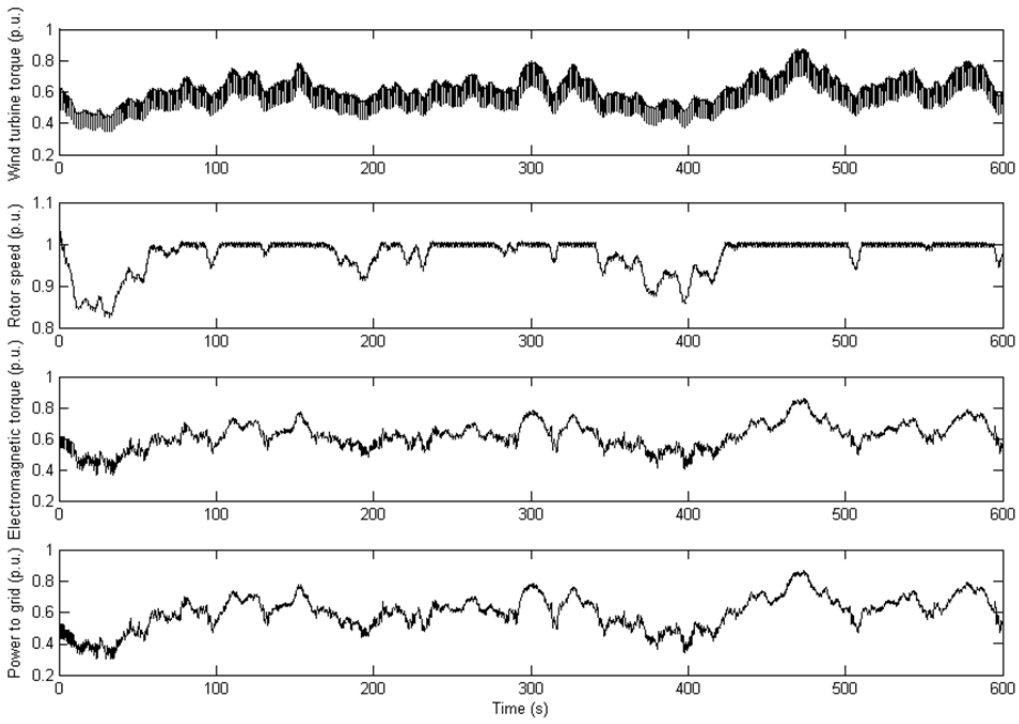

A frequency analysis of the output active power into the grid has been carried out, as shown in Figure 10. Compared with the frequency analysis of the output active power into the grid without FMSC (see Figure 4), the 3p oscillation frequency components, which are the significant parts in the

flicker emission of variable wind speed turbines with PMSG during continuous operation, are damped evidently. As a consequence, the flicker mitigation may be realized using FMSC.

Figure 11 illustrates the variation of short-term flicker severity P_{st} with mean wind speed between the case without FMSC and the case with FMSC. It can be concluded that damping the 3p active power oscillation due to wind shear and tower shadow effects by using the FMSC is an effective means for flicker mitigation of variable speed wind turbines with PMSG during continuous operation at different mean wind speed.

This proposed control method uses the existing large inertia of the wind turbine rotor as the storage of the fluctuation power instead of the big DC-link capacitor as suggested in [15]. The total cost of the system using the proposed method is considered to be lower than the cost using the method in [15]. Since both control methods use different components as the storage of the fluctuation power, the combination of both control methods may give a lower flicker level.

Figure 10. Power spectral density (PSD) of the output active power of the wind turbine with FMSC.

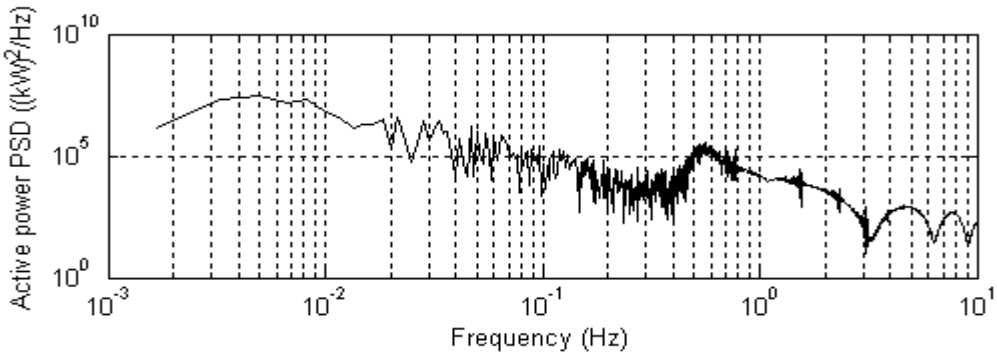

Figure 11. The variation of short-term flicker severity P_{st} with mean wind speed between the case without FMSC (asterisk) and the case with FMC (diamond).

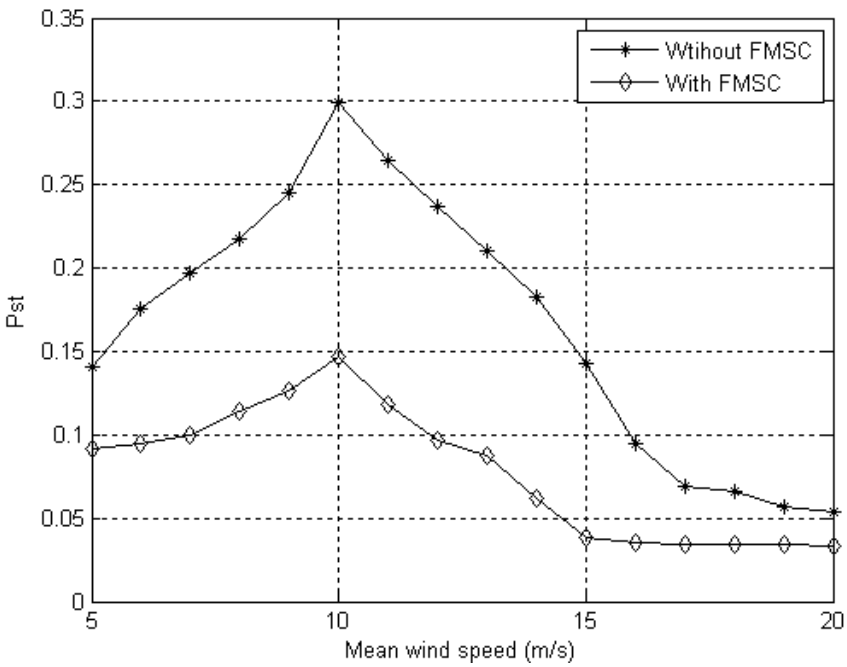

6. Conclusions

This paper describes a method of flicker mitigation by speed control of variable speed wind turbines with full-scale back-to-back power converters and PMSG. The model of a MW-level variable speed wind turbines with PMSG using the full-scale back-to-back PWM voltage source converters and the corresponding control schemes are described in this paper. On the basis of the developed wind turbine model, the flicker emissions of this system are investigated. Flicker mitigation may be realized by using the flicker mitigation controller to damp the 3p active power oscillation due to wind shear and tower shadow effects which is significant in the flicker emission. A new controller for flicker mitigation by speed control is proposed. The FMSC smoothes the 3p active power oscillations from wind shear and tower shadow effects of the wind turbine by varying the rotational speed of the PMSG. It can be concluded from the simulation results that damping the 3p active power oscillation by using the FMSC is an effective means for flicker mitigation of variable speed wind turbines with full-scale back-to-back power converters during continuous operation.

Acknowledgments

This work was supported by the Danish Agency for Science, Technology and Innovation, project DSF-09-071588 "Dynamic wind turbine model-from wind to grid".

Conflict of Interest

The authors declare no conflict of interest.

Appendix

Table A1. The Parameters of The Variable Speed Wind Turbine with PMSG.

Parameter	Value	Parameter	Value
Rated power	2 MW	Distance from the blade origin to the tower midline(x)	4 m
Rated voltage	0.69 kV	Angular moment of wind turbine inertia	2.5 s
Rated speed	15.5 rpm	Angular moment of PMSG inertia	0.2 s
Stator resistance	0.03 p.u.	Drive train shaft stiffness	30 p.u.
Stator direct reactance (X_d)	0.775 p.u.	Turbulence intensity ($In = \Delta v / v$)	0.1
Stator quadrature reactance (X_q)	0.775 p.u.	Rated power of the transformer	2.5 MVA
Stator leakage inductance	0.064 p.u.	Rated voltage of primary winding of the transformer	11 kV
Magnetic strength	1 p.u.	Rated voltage of secondary winding of the transformer	0.69 kV
Wind turbine rotor radius	40 m	Leakage reactance of the transformer	0.04 p.u.
Elevation of rotor hub	80 m	Impedance magnitude of line 1–2	0.7562 Ω
Empirical wind shear exponent (α)	0.3	Short circuit capacity ratio ($SCR = S_k/S_n$)	10
Tower radius (a)	2 m	Grid impedance angle (ψ_k)	60 degree

Notes: Δv is the wind speed standard deviation; v is the mean wind speed; S_k is the short circuit apparent power of the grid where the wind turbines are connected; S_n is the rated apparent power of the wind turbines.

References

1. Rossetto, L.; Tenti, P.; Zuccato, A. Electromagnetic compatibility issues in industrial equipment. *IEEE Ind. Appl. Mag.* **1999**, *5*, 34–46.
2. Chinchilla, M.; Arnaltes, S.; Burgos, J.C. Control of permanent-magnet generators applied to variable-speed wind-energy systems connected to the grid. *IEEE Trans. Energy Convers.* **2006**, *21*, 130–135.
3. Larsson, A. Flicker emission of wind turbines during continuous operation. *IEEE Trans. Energy Convers.* **2002**, *17*, 114–118.
4. Sharma, H.; Islam, S.; Pryor, T.; Nayar, C.V. Power quality issues in a wind turbine driven induction generator and diesel hybrid autonomous grid. *J. Elect. Electron. Eng.* **2001**, *21*, 19–25.
5. Papadopoulos, M.P.; Papathanassiou, S.A.; Tentzerakis, S.T.; Boulaxis, N.G. Investigation of the Flicker Emission by Grid Connected Wind Turbines. In Proceedings of 8th International Conference on Harmonics Quality of Power, Athens, Greece, 14–18 October 1998; pp. 1152–1157.
6. Hu, W.; Chen, Z.; Wang, Y.; Wang, Z. Flicker Study on Variable Speed Wind Turbines with Permanent Magnet Synchronous Generator. In Proceedings of 13th Power Electronics and Motion Control Conference (EPE-PEMC), Poznan, Poland, 1–3 September 2008; pp. 2325–2330.
7. Sun, T.; Chen, Z.; Blaabjerg, F. Flicker study on variable speed wind turbines with doubly fed induction generators. *IEEE Trans. Energy Convers.* **2005**, *20*, 896–905.
8. Hill, J.E. A practical example of the use of distribution static compensator (D-STATCOM) to reduce voltage fluctuation. In Proceedings of the IEE Colloquium on Power Electronics for Renewable Energy, London, UK, 16 June 1997; pp. 711–715.
9. Mohod, S.W.; Aware, M.V. A STATCOM-control scheme for grid connected wind energy system for power quality improvement. *IEEE Syst. J.* **2010**, *4*, 346–352.
10. Kasem, A.H.; El-Saadany, E.F.; El-Tamaly, H.H.; Wahab, M.A.A. Power ramp rate control and flicker mitigation for directly grid connected wind turbines. *IET Renew. Power Gener.* **2010**, *4*, 261–271.
11. Ammar, M.; Joos, G. Impact of distributed wind generators reactive power behavior on flicker severity. *IEEE Trans. Energy Convers.* **2013**, *28*, 425–433.
12. Kim, Y.S.; Won, D.J. Mitigation of the flicker level of a DFIG using power factor angle control. *IEEE Trans. Power Deliv.* **2009**, *24*, 2457–2458.
13. Yazdani, A.; Crow, M.L.; Guo, J. An improved nonlinear STATCOM control for electric arc furnace voltage flicker mitigation. *IEEE Trans. Power Deliv.* **2009**, *24*, 2284–2290.
14. Scott, N.C.; Atkinson, D.J.; Morrell, J.E. Use of load control to regulate voltage on distribution networks with embedded generation. *IEEE Trans. Power Syst.* **2002**, *17*, 510–515.
15. Hu, W.; Chen, Z.; Wang, Y.; Wang, Z. Flicker mitigation by active power control of variable-speed wind turbines with full-scale back-to-back power converters. *IEEE Trans. Energy Convers.* **2009**, *24*, 640–649.
16. Rosas, P.A.C.; Sørensen, P.; Bindner, H. Fast Wind Modeling for Wind Turbines. In Proceedings of Wind Power 21st Century EUWER Special Topic Conference and Exhibition, Kassel, Germany, 25–27 September 2000; pp. 184–187.

17. Dolan, D.S.L.; Lehn, P.W. Simulation model of wind turbine 3p torque oscillations due to wind shear and tower shadow. *IEEE Trans. Energy Convers.* **2006**, *21*, 717–724.
18. Petru, T.; Thiringer, T. Modeling of wind turbines for power system studies. *IEEE Trans. Power Syst.* **2002**, *17*, 1132–1139.
19. Canay, I.M. Causes of discrepancies on calculation of rotor quantities and exact equivalent diagrams of the synchronous machine. *IEEE Trans. Power Appar. Syst.* **1969**, *88*, 1114–1120.
20. Giroux, P.; Sybille, G.; Le-Huy, H. Modeling and Simulation of a Distribution STATCOM Using Simulink's Power System Blockset. In Proceedings of 27th Annual Conference IEEE Industrial Electronics Society, Denver, CO, USA, 29 November–2 December 2001; pp. 990–994.
21. Moor, G.D.; Beukes, H.J. Maximum Power Point Trackers for Wind Turbines. In Proceedings of 35th Annual IEEE Power Electronics Specialists Conference, Aachen, Germany, 20–25 June 2004; pp. 2044–2049.
22. Burton, T.; Sharpe, D.; Jenkins, N.; Bossanyi, E. *Wind Energy Handbook*; John Wiley and Sons: Hoboken, NJ, USA, 2001.
23. Senjyu, T.; Shimabukuro, T.; Uezato, K. Vector Control of Permanent Magnet Synchronous Motors without Position and Speed Sensors. In Proceedings of 26th Annual IEEE Power Electronics Specialists Conference, Atlanta, GA, USA, 18–22 June 1995; pp. 759–765.
24. Chen, Z.; Guerrero, J.M.; Blaabjerg, F. A review of the state of the art of power electronics for wind turbines. *IEEE Trans. Power Electron.* **2009**, *24*, 1859–1875.
25. Li, S.; Haskew, T.A.; Swatloski, R.P.; Gathings, W. Optimal and direct-current vector control of direct-driven PMSG wind turbines. *IEEE Trans. Power Electron.* **2012**, *27*, 2325–2337.
26. Rodriguez, P.; Timbus, A.; Teodorescu, R.; Liserre, M.; Blaabjerg, F. Reactive power control for improving wind turbine system behavior under grid faults. *IEEE Trans. Power Electron.* **2009**, *24*, 1798–1801.
27. Uehara, A.; Pratap, A.; Goya, T.; Senjyu, T.; Yona, A.; Urasaki, N.; Funabashi, T. A coordinated control method to smooth wind power fluctuations of a PMSG-Based WECS. *IEEE Trans. Energy Convers.* **2011**, *26*, 550–558.
28. Haque, M.E.; Negnevitsky, M.; Muttaqi, K.M. A novel control strategy for a variable-speed wind turbine with a permanent-magnet synchronous generator. *IEEE Trans. Ind. Appl.* **2010**, *46*, 331–339.
29. *IEEE Recommended Practice—Adoption of IEC 61000-4-15: Electromagnetic Compatibility (EMC)—Testing and Measurement Techniques—Flickermeter—Functional and Design Specifications*; IEEE Std 1453-2011-Redline; IEEE: New York, NY, USA, 2011; pp. 1–89.
30. The MathWorks Home Page. Available online: http://www.mathworks.com/ (accessed on 10 February 2013).